Circuits and Systems, 2022, 13, 1-12
https://www.scirp.org/journal/cs
ISSN Online: 2153-1293
ISSN Print: 2153-1285

Behavioral Model of Molecular Gap-Type Atomic Switches and Its SPICE Integration

Hiroshi Kubota[1*], Tsuyoshi Hasegawa[2], Megumi Akai-Kasaya[1], Tetsuya Asai[1]

[1]Graduate School of Information Science and Technology, Hokkaido University, Sapporo, Japan
[2]School of Advanced Science and Engineering, Waseda University, Tokyo, Japan
Email: *kubota.hiroshi.ik@ist.hokudai.ac.jp

How to cite this paper: Kubota, H., Hasegawa, T., Akai-Kasaya, M. and Asai, T. (2022) Behavioral Model of Molecular Gap-Type Atomic Switches and Its SPICE Integration. *Circuits and Systems*, **13**, 1-12.
https://doi.org/10.4236/cs.2022.131001

Received: December 2, 2021
Accepted: January 27, 2022
Published: January 30, 2022

Copyright © 2022 by author(s) and Scientific Research Publishing Inc.
This work is licensed under the Creative Commons Attribution International License (CC BY 4.0).
http://creativecommons.org/licenses/by/4.0/

Open Access

Abstract

Atomic switches can be used in future nanodevices and to realize conceptually novel electronics in new types of computer architecture because of their simple structure, ease of operation, stability, and reliability. The atomic switch is a single solid-state switch with inherent learning abilities that exhibits various nonlinear behaviors with network devices. However, previous studies focused on experiments and nonvolatile memory applications, and studies on the application of the physical properties of the atomic switch in computing were nonexistent. Therefore, we present a simple behavioral model of a molecular gap-type atomic switch that can be included in a simulator. The model was described by three simple equations that reproduced the bistability using a double-well potential and was able to easily be transferred to a simulator using arbitrary numerical values and be integrated into HSPICE. Simulations using the experimental parameters of the proposed atomic switch agreed with the experimental results. This model will allow circuit designers to explore new architectures, contributing to the development of new computing methods.

Keywords

Memristor, Atomic Switch, Behavioral Model, SPICE

1. Introduction

Atomic switches are a new type of nanodevices [1]. Recently, atomic switches have been developed for nonvolatile memory devices. Typically, they are generated simply by crossing Pt wires and Ag_2S-coated Ag wires and can be created with materials such as Cu_2S [2] [3]. Atomic switches can be controlled by applying a voltage between the electrodes, and their switching characteristics can be switched on and off at room temperature and in the air [4]-[9]. In addition,

atomic switches have a large ratio of the highest resistance state to the lowest resistance state and can maintain their states for more than a week [10] [11]. Their working speeds are as fast as those of conventional electronic devices, and this will enable the development of a new type of computer architecture beyond von Neumann computers [12] [13] [14]. Atomic switches have the characteristic of a memristor, which means that devices memorize the input voltage, and the resistance of the device decreases as the number of inputs increases or the input interval is short [15] [16] [17]. Because atomic switches have synapse-like characteristics, their network hardware, which consists of neuromorphic devices such as reservoirs, has been studied [18] [19] [20] [21] [22]. Physical and chemical phenomena occurring in atomic switches, such as redox reactions, ion diffusion, and their nucleation, have also been studied both theoretically and experimentally [23] [24] [25]. Experiments on atomic switches in physics, nonvolatile memory applications such as programmable buses, applications as a randomly generated circuit [26] [27], and equations in physics have been proposed, but there has been no research on the circuit models for SPICE. Hence, the precise physical model of the atomic switch is required, however, before completion of the precise model, a behavioral model of atomic switches that can easily be used in SPICE is also required by circuit engineers developing memristor-based novel circuits and systems, aiming at exploring novel values of memristors, instead of optimizing circuit performances by using precise physical models. In this paper, we propose simple differential equations that relate the input voltage of an atomic switch to the resistance of the device. These equations were added to HSPICE. This enables engineers, mathematicians, and circuit designers who have not used these devices until now, for example, to explore new computing methods. When voltage is applied to a molecular gap-type atomic switch, the number of ions in the electrode is reduced, and atoms are deposited in the gap between the electrodes. This switch has two states: one in which a metal filament grows between the electrodes, and the other in which the filament growth is completed and the filament that bridges the two electrodes becomes stable. This bistability is represented by a double potential well, which can represent the states of metal atoms between electrodes as an equation. In addition, we developed an equation for metal ions in the electrode and mapped the states of metal atoms and device resistances. Device operations can be described using these equations.

2. Behavioral Model of Atomic Switches

The equations represent the qualitative behavior of these atomic switches. When voltage is applied to this element, metal ions drift to the negative side of the electrode and deposit as atoms between the electrodes, causing an element resistance change.

2.1. Ion Density Gradient

The deposition of atoms is caused by the reduction in the number of ions, and

the electrochemical potential of ions in the electrode changes the deposition speed [28]. We used molecular gap atomic switches with one electrode containing ions and the other without ions. We introduced a variable σ_r that shows the entire status with respect to the ion shift in the electrode when voltage is applied. σ_r is positive when the electrochemical potential of ions advances the atom deposition; otherwise, it is negative and is described as

$$\tau_r \dot{\sigma}_r = -(\sigma_r - \alpha v), \tag{1}$$

where v is the applied voltage, alpha is the gain, and τ_r is the time constant. This equation gives the value of σ_r as per αv with a time delay.

2.2. Growth of Metal Filament

Deposited atoms form a metal filament that grows from a positively biased electrode to a negatively biased electrode, forming a bridge between the electrodes. Under reduced or reversed voltages, the atoms are ionized and dissolved into the electrode, where they initially existed. An atomic switch has two stable states: an OFF state in which ions exist in an electrode under lower voltage, and an ON state in which the bridge formation is completed. These two states are stable even after removing applied bias. This demonstrates bistability. However, if the ON state element is applied with reversed voltage over the threshold, it changes to the OFF state [27].

The status of an atomic filament is represented by variable σ_0. We assume that the bistable dynamics are obtained by the following double-well function:

$$H(\sigma_0) \equiv \frac{\sigma_0^4}{4} - \frac{(\sigma_0 - V_d)^2}{2} - \sigma_0 f_{\text{ext}}(\sigma_r), \tag{2}$$

where σ_0 represents the two states ON/OFF ($\sigma_0 \geq 1/\sqrt{3}$: ON and $\sigma_0 \leq -1/\sqrt{3}$: OFF).

$f_{\text{ext}}(\sigma_r)$ is the external force, which is a function of σ_r [because the deposition or ionization of the bridging atoms is dominated by the electrochemical potential of ions (σ_r)].

V_d is a constant representing the asymmetry of the amounts of the external forces [$f_{\text{ext}}(\sigma_r)$] for ON → OFF and OFF → ON transitions. From the stable condition given by $\mathrm{d}\sigma_0/\mathrm{d}t = -\nabla H$, we obtain

$$\tau_0 \dot{\sigma}_0 = -\left(\sigma_0^3 - (\sigma_0 - V_d) - f_{\text{ext}}(\sigma_r)\right), \tag{3}$$

where τ_0 is a time constant, which is time dependent. We define $f_{\text{ext}}(\sigma_r) \equiv p\sigma_r$, where p (>0) is a constant.

In Equation (3), when the condition is $-2\times 3^{-1.5} \leq \sigma_r - V_d$, the state changes from the OFF state to the ON state; and when the condition is $-2\times 3^{-1.5} \geq \sigma_r - V_d$, the state changes from the ON state to the OFF state. In addition, in Equation (1), $\sigma_r = \alpha v$ when time passes. Hence, we obtain

$$\alpha = \frac{4}{3\sqrt{3}} \frac{1}{V_{\text{on}} - V_{\text{off}}}, \tag{4}$$

$$V_d = \frac{2}{3\sqrt{3}} \frac{V_{on} + V_{off}}{V_{on} - V_{off}}, \quad (5)$$

where V_{on} is the OFF → ON threshold voltage, and V_{off} is the ON → OFF threshold voltage.

2.3. Equation of Resistance

The atom deposition changes the element resistance, and the resistance exponentially decreases with an increase in the number of atoms deposited between the electrodes. Therefore, the resistance function $R(\sigma_0)$ is defined by the exponential function as

$$R(\sigma_0) \equiv k_R \exp\{-\beta \times f(\sigma_0)\}, \quad (6)$$

where k_R and β are the fitting parameters, and $f(\sigma_0)$ is a monotonically increasing function that represents high resistance when σ_0 is negative and low resistance when σ_0 is positive.

3. Experimental and Simulation Results

3.1. Target Device and Features

Pt/PTCDA[1]/Ta_2O_5/Ag molecular atomic switch is our target device [**Figure 1(a)**] [27]. It is composed of Ag (active electrode), Ta_2O_5 (ionic transfer layer), PTCDA (gap layer), and Pt (inert electrode). When a positive voltage is applied to the Ag electrode, Ag^+ ions move in the transfer layer toward the gap layer and deposit as Ag atoms that subsequently bridge the gap.

Figure 1(b) shows the V–I characteristics of this device. Voltage is applied to the bottom electrode as 0 V → 0.3 V → −0.3 V → 0 V with a compliance current of 50 μA. Initially, the atomic switch was in the OFF state, then it changed to the ON state at 0.29 V and reset to the ON state at −0.16 V. We extracted the parameter values of V_{off} and V_{on}, which are the threshold voltages that cause transitions of the device states in Equations (4) and (5), from **Figure 1(b)** as $V_{off} = -0.16$ V, $V_{on} = 0.29$ V.

Figure 1(c) and **Figure 1(d)** show the behavior of another device under the application of voltage pulses (0.36 V in height and 1.0 s. in width) at different intervals of (c) 4.0 s and (d) 1.0 s. Short-interval pulses can change an OFF state device to the ON state, but long interval pulses cannot.

The measurement method and the conditions were the same as in this paper [27].

3.2. Determination of Resistance Function

We defined the OFF state as $\sigma_0 < s_{th}$, the ON state as $\sigma_0 > s_{th}$, where s_{th} is the local maximum of $H(\sigma_0)$ representing the peak of the intervening barrier when $f_{ext}(\sigma_r) = 0$, as shown in the upper part of **Figure 2**, R_{high} as the high resistance when the device is OFF state, and R_{low} as the low resistance when

[1]N,N'-Dioctyl-3,4,9,10-Perylenedicarboximide.

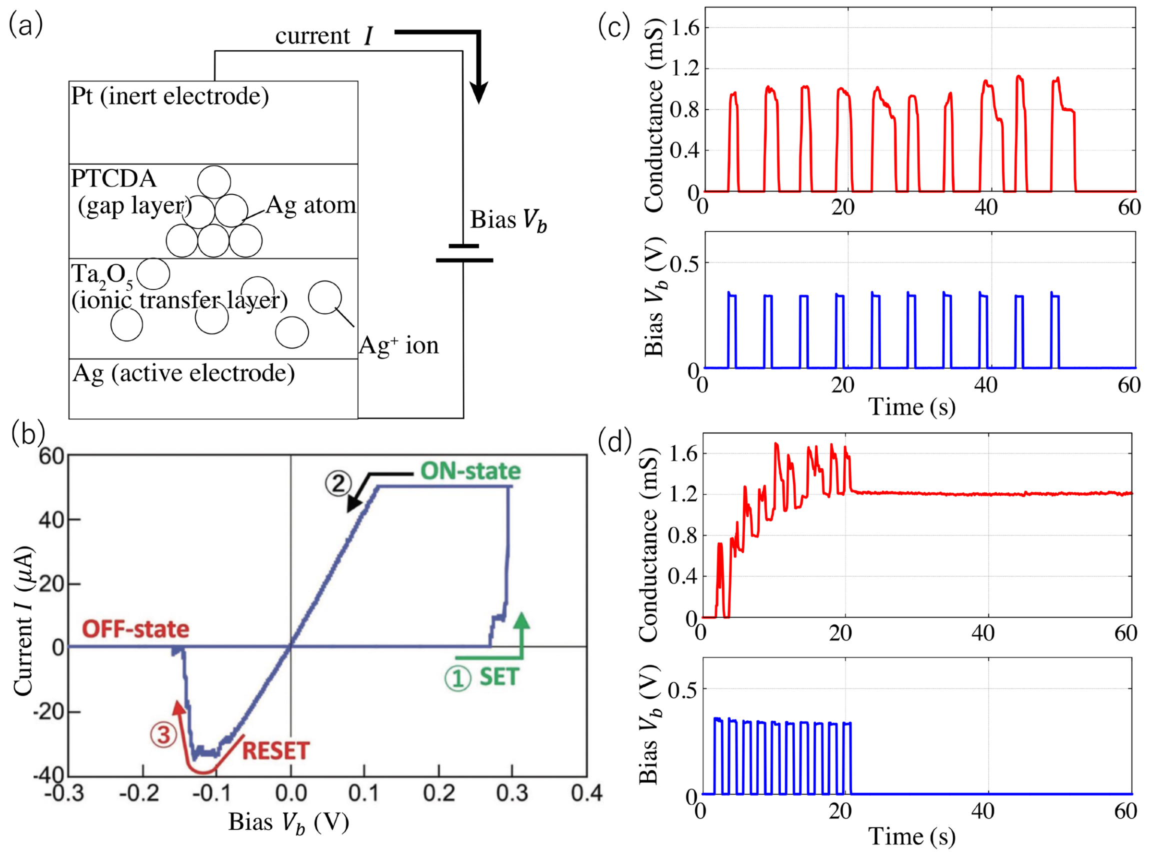

Figure 1. (a) Target atomic switch device. (b) V-I characteristics of device (John Wiley and Sons, license # 5255060486672) (c) and (d) Conductance of device when 10 pulses are applied in the atomic switch. Pulse heights, widths, and intervals of (c) are 0.36 V, 1.0 s, and 4.0 s; and (d) 0.36 V, 1.0 s, and 1.0 s, respectively [27].

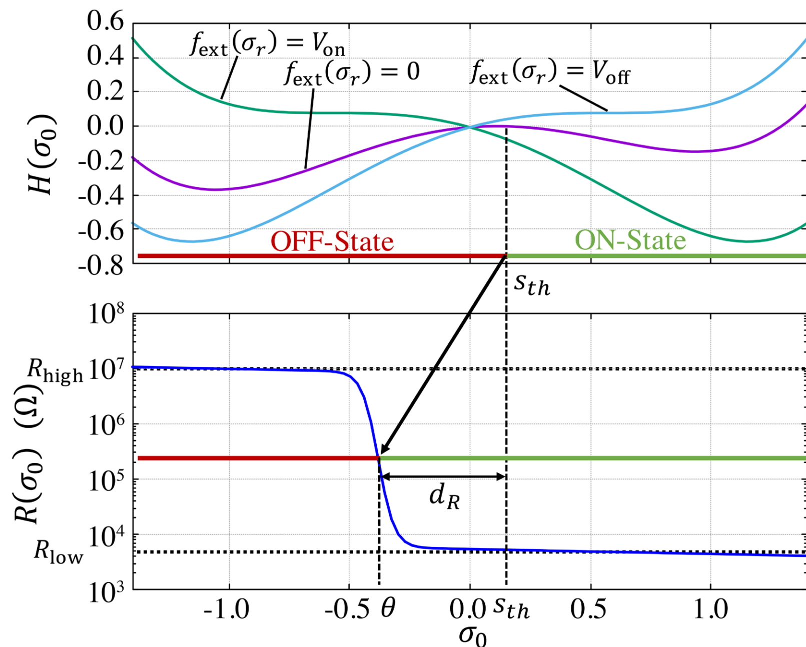

Figure 2. Potential $H(\sigma_0)$ [Equation (2)] and device resistance function $R(\sigma_0)$ [Equation (6) with Equation (7)] vs. σ_0.

the device is ON state. In addition, we assume that the monotonically increasing function $f_{\text{ext}}(\sigma_r)$ as a function of the device resistance [Equation (6)] is a resistance function that changes smoothly with σ_0; hence, we used a hyperbolic tangent function. In addition, $R(\sigma_0)$ decreases as σ_0 increases, which is the filament growth; thus, we used a linear increasing function. To sum up, we defined $f(\sigma_0)$ in Equation (6) as follows:

$$f(\sigma_0) \equiv (\sigma_0 - \theta) \times g_R + \tanh\{(\sigma_0 - \theta) \times s_R\}, \tag{7}$$

where θ is the inflection point value in $f(\sigma_0)$, $g_R(>0)$ is the gradient of the linear increasing function, and s_R is the gradient at the inflection point in $f(\sigma_0)$. The parameters θ and s_R are defined below.

First, parameter θ is explained as follows. As shown in **Figure 1(c)** (changes in the conductance of the atomic switch device in its OFF state with periodic voltage pulse inputs), the device is not completely turned on (the conductance is temporarily increased at the pulse onset [positive pulse amplitude], but suddenly decreased to zero when the pulse amplitude becomes zero). However, the conductance is significantly changed, that is, the device resistance changes between R_{high} and R_{low} even though the device remains in the OFF state. Therefore, s_{th} cannot directly represent the resistance change inflection points.

Here, we introduce two new parameters—θ, representing the resistance change inflection point, as shown in the lower part of **Figure 2**, and d_R, representing the difference between the threshold value of the ON/OFF state transition (s_{th}) and θ, that is, $d_R \equiv s_{th} - \theta$.

Second, the parameter g_R is explained. **Figure 1(d)** shows that the device resistance decreases when pulses are applied, even after the transition to the ON state. Because $f(\sigma_0) \approx (\sigma_0 - \theta) \times g_R + 1$ in the ON state and the increase in σ_0 with pulse input increases $f(\sigma_0)$ [decreasing $R(\sigma_0)$], we can fit the parameter values of θ and/or g_R with the experimental results. For simplicity, we chose g_R as the tuning parameter.

In our simulations, we determined the parameters $s_R = 15$ and $\theta = -0.38$. When $f(\sigma_0)$ is defined and the parameters of are determined as outlined above,

$$R_{\text{high}} = R(-1) \approx k_R \exp\left[-\beta\{(-1-\theta) \times g_R - 1\}\right], \tag{8}$$

$$R_{\text{low}} = R(0) \approx k_R \exp\{-\beta(-\theta \times g_R + 1)\} \tag{9}$$

are derived.

We determined $R_{\text{high}} = 10\ \text{M}\Omega$ because when the gap layer has no atoms, the tunneling current flow and the device resistance are approximately 10 MΩ. We determined R_{low} from experimental results. From this, we obtained the following parameters:

$$\beta = \frac{\log\left(\frac{R_{\text{high}}}{R_{\text{low}}}\right)}{g_R + 2}, \quad k_R = R_{\text{high}} \exp\left[-\beta\{(1+\theta) \times g_R + 1\}\right]. \tag{10}$$

The lower part of **Figure 2** shows this resistance curve as outlined above with

$\theta = -0.38$, $g_R = 0.1$, $s_R = 15$, $R_{\text{high}} = 10\ \text{M}\Omega$, and $R_{\text{low}} = 2.8\ \text{k}\Omega$.

3.3. HSPICE Netlists

Figure 3 shows HSPICE netlists of our atomic switch model based on Equations (1), (3), and (6) with Equation (7). Figure 3(a) is the atomic switch subcircuit.

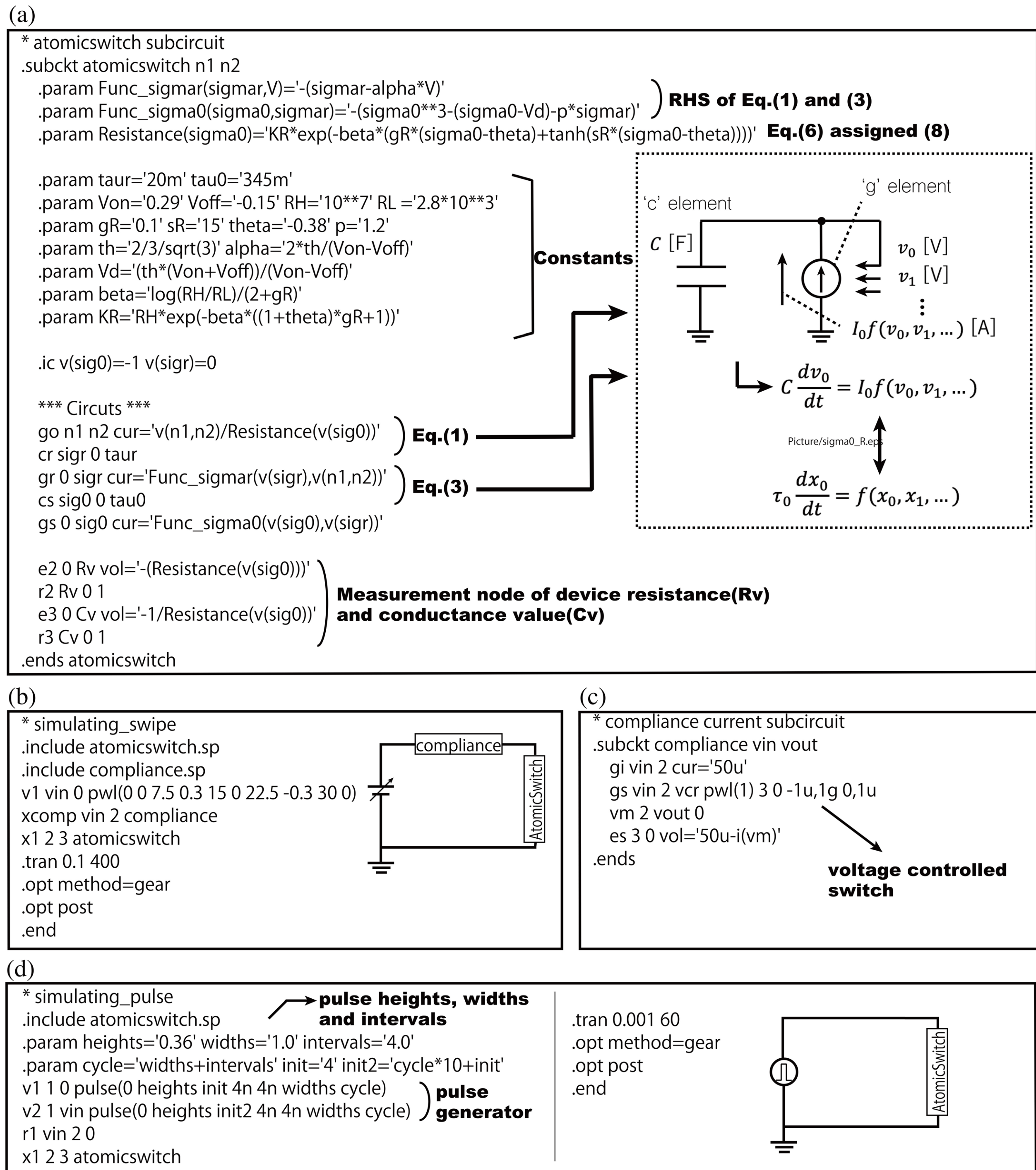

Figure 3. HSPICE netlists of behavioral atomic switch model. (a) Atomic switch subcircuit. (b) Simulation circuit for V-I characteristics. (c) Subcircuit of compliance current. (d) Simulation circuit with pulses.

Both differential Equations (1) and (3) are represented by a circuit of capacitors ("c" elements) and voltage-controlled current source ("g" elements). Details for implementing ordinary differential equations in SPICE can be found in the general guidelines [29] [30]. The device parameters were defined as variables in ".params". The ends of the device are nodes "n1" and "n2". The resistance was represented by a current source that supplies $V_{n1,n2}/R(\sigma_0)$, where $V_{n1,n2}$ is the voltage applied to the device, and $R(\sigma_0)$ is the resistance of the device calculated in this subcircuit.

Figure 3(b) shows the test circuit for simulating the V-I characteristics of the atomic switch model. In this simulator, the input voltage transition changes linearly with 0 V → 0.3 V → −0.3 V → 0 V with a compliance current of 50 μA. The compliance current is provided by the subcircuit shown in **Figure 3(c)**. The subcircuit has a 50 μA current source and a voltage-controlled switch. This switch is off when 50 μA minus the value of the flowing current in this subcircuit element is negative, otherwise, it is on. This means that the current value flowing in this subcircuit is limited to 50 μA; otherwise, all the current flows through this element.

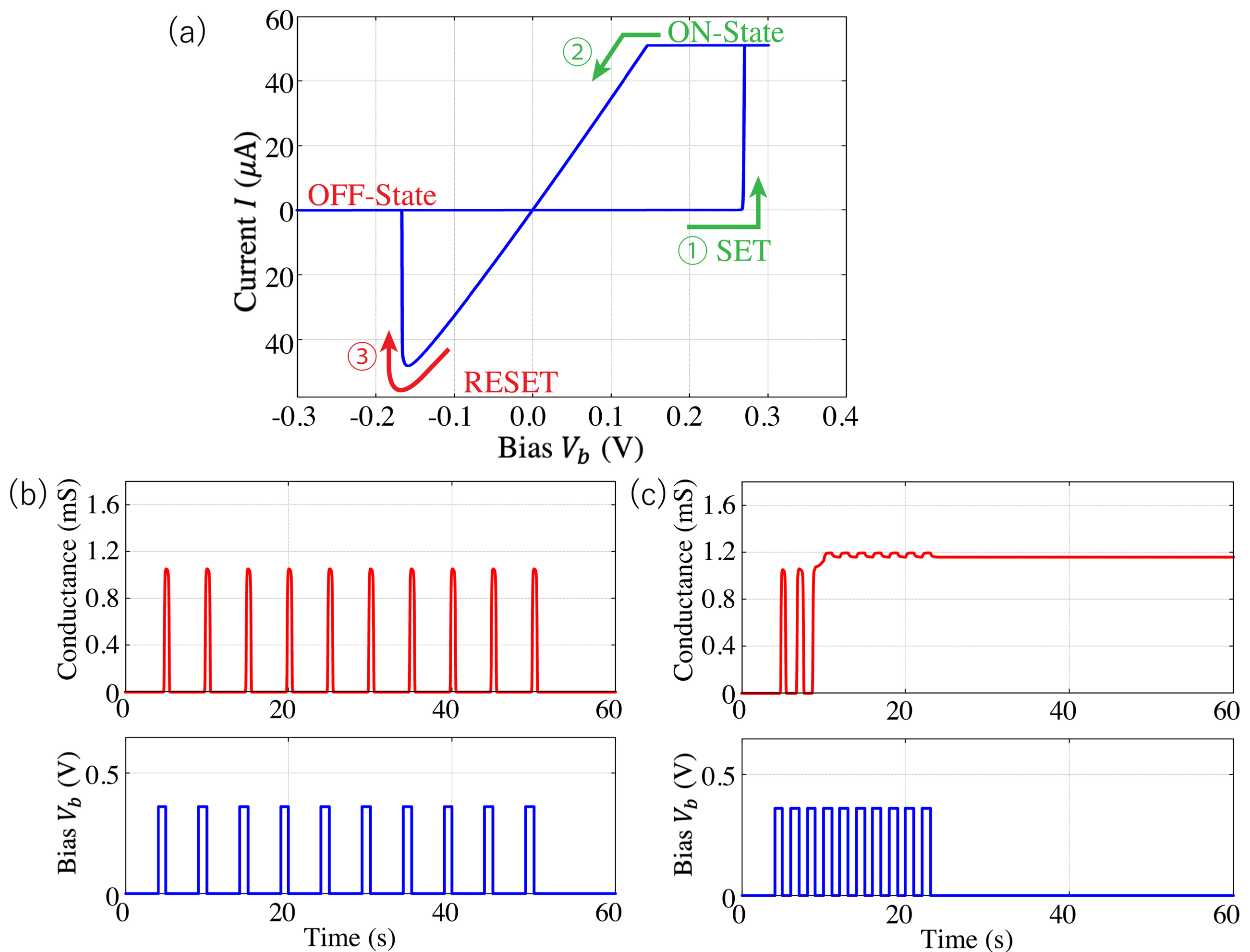

Figure 4. (a) Simulation result for V-I characteristic. Initially, OFF state is set and it is changed to ON state at 0.29 V and reset and changed to OFF state at −0.16 V. (b)-(c) Simulation results of device conductance with input pulses. Pulse heights, widths, and intervals of (b) are 0.36 V, 1.0 s, and 4.0 s; and (c) 0.36 V, 1.0 s, and 1.0 s, respectively.

Figure 3(d) is a pulse response simulator circuit with height, width, and interval of 0.36 V, 1.0 s and 4.0 s, respectively. This subcircuit was simulated with a variety of heights, widths, and intervals by changing the top ".param" card.

3.4. Simulation Results

In the simulations shown in **Figures 4(a)-(c)**, we set $\theta = -0.38$, $g_R = 0.1$, $s_R = 15$, $p = 1.2$, $\tau_r = 20\text{ ms}$, and $\tau_0 = 345\text{ ms}$. **Figure 4(a)** shows the results of our atomic switch model simulated by **Figure 4(b)**, which provides the netlist, similar to **Figure 4(b)**. We extracted R_{low} from **Figure 1(b)** as $R_{\text{low}} = 2.8\text{ k}\Omega$. This indicates that our model has two states: it changes from the OFF state to the ON state at 0.29 V and returns from the ON state to the OFF state at approximately −0.16 V. Each state has a different resistance.

We simulated this model with a pulse whose height, width, and interval in (b) are 0.36 V, 1.0 s, and 4.0 s; and (c) are 0.36 V, 1.0 s, and 1.0 s. In **Figure 4(b)** and **Figure 4(c)**, we simulated our model with each pulse condition from **Figure 1(c)** and **Figure 1(d)**, which are the different interval pulse inputs. We extracted R_{low} from **Figure 1(d)** as $R_{\text{low}} = 830\ \Omega$. When different interval pulses are applied, we obtain different transitions, which remain in the OFF state with longer interval pulses and change to the ON state with shorter interval pulses.

4. Conclusions

We proposed a behavioral model of a molecular gap-type atomic switch. It was described by two differential equations and a nonlinear function and can be integrated into a circuit simulator. We integrated on HSPICE, and the simulation represented the device characteristics. This showed two states and a pulse-dependent change. The results agreed with the experimental results for a molecular gap-type atomic switch.

By using the proposed model, various circuit engineers can use a novel nonlinear, nonvolatile memory device in their research, which may accelerate exploring new architectures for nonvolatile memory-array circuits, expansion of nonlinear science that exploits nonlinear dynamics of atomic switches as well as novel computing architectures. For example, a novel reservoir computing on an elementary model of atomic switches with high precision and excellent memory characteristics has already been proposed [31], which implies that the proposed behavioral model will be useful for exploring the extension of various analog and digital circuits and systems.

Acknowledgements

This work is partly based on the results obtained from a project (JPNP16007) subsidized by the New Energy and Industrial Technology Development Organization (NEDO).

Conflicts of Interest

The authors declare no conflicts of interest regarding the publication of this paper.

References

[1] Eigler, D.M., Lutz, C.P. and Rudge, W.E. (1991) An Atomic Switch Realized with the Scanning Tunnelling Microscope. *Nature*, **352**, 600-603. https://doi.org/10.1038/352600a0

[2] Terabe, K., Hasegawa, T., Nakayama, T. and Aono, M. (2005) Quantized Conductance Atomic Switch. *Nature*, **433**, 47-50. https://doi.org/10.1038/nature03190

[3] Nayak, A., Tsuruoka, T., Terabe, K., Hasegawa, T. and Aono, M. (2011) Theoretical Investigation of Kinetics of a Cu_2S-Based Gap-Type Atomic Switch. *Applied Physics Letters*, **98**, Article ID: 233501. https://doi.org/10.1063/1.3597154

[4] Terabe, K., Hasegawa, T., Nakayama, T. and Aono, M. (2001) Quantum Point Contact Switch Realized by Solid Electrochemical Reaction. *Riken Review*, **37**, 7-8. https://doi.org/10.7567/SSDM.2001.D-8-3

[5] Tamura, T., Hasegawa, T., Terabe, K., Nakayama, T., Sakamoto, T., Sunamura, H., Kawaura, H., Hosaka, S. and Aono, M. (2007) Material Dependence of Switching Speed of Atomic Switches Made from Silver Sulfide and from Copper Sulfide. *Journal of Physics*: *Conference Series*, **61**, 1157-1161. https://doi.org/10.1088/1742-6596/61/1/229

[6] Waser, R. and Aono, M. (2007) Nanoionics-Based Resistive Switching Memories. *Nature Materials*, **6**, 833-840. https://doi.org/10.1038/nmat2023

[7] Smith, D.P.E. (1995) Quantum Point Contact Switches. *Science*, **269**, 371-373. https://doi.org/10.1126/science.269.5222.371

[8] Sakamotoa, T., Listerb, K. and Banno, N. (2007) Electronic Transport in Ta_2O_5 Resistive Switch. *Applied Physics Letters*, **91**, Article ID: 092110. https://doi.org/10.1063/1.2777170

[9] Pascual, J.I., Méndez, J., Gómez-Herrero, J., Baró, A.M., Garcia, N. and Binh, Vu Thien, B. (1993) Quantum Contact in Gold Nanostructures by Scanning Tunneling Microscopy. *Physical Review Letters*, **71**, 1852-1855. https://doi.org/10.1103/PhysRevLett.71.1852

[10] Wu, S., Tsuruoka, T., Terabe, K., Hasegawa, T., Hill, J.P., Ariga, K. and Aono, M. (2011) A Polymer-Electrolyte-Based Atomic Switch. *Advanced Functional Materials*, **21**, 93-99. https://doi.org/10.1002/adfm.201001520

[11] Tada, M., Sakamoto, T., Banno, N., Aono, M., Hada, H. and Kasai, N. (2010) Nonvolatile Crossbar Switch Using $TiO_x/TaSiO_y$ Solid Electrolyte. *IEEE Transactions on Electron Devices*, **57**, 1987-1995. https://doi.org/10.1109/TED.2010.2051191

[12] Tamura, T., Hasegawa, T., Terabe, K., Nakayama, T., Sakamoto, T., Sunamura, H., Kawaura, H., Hosaka, S. and Aono, M. (2006) Switching Property of Atomic Switch Controlled by Solid Electrochemical Reaction. *Japanese Journal of Applied Physics*, **45**, L364-L366. https://doi.org/10.1143/JJAP.45.L364

[13] Tsuruoka, T., Hasegawa, T., Terabe, K. and Aono, M. (2017) Operating Mechanism and Resistive Switching Characteristics of Two- and Three-Terminal Atomic Switches Using a Thin Metal Oxide Layer. *Journal of Electroceramics*, **39**, 143-156. https://doi.org/10.1007/s10832-016-0063-9

[14] Demis, E.C., Aguilera, R., Sillin, H.O., Scharnhorst, K., Sandouk, E.J., Aono, M., Stieg, A.Z. and Gimzewski, J.K. (2015) Atomic Switch Networks—Nanoarchitectonic Design of a Complex System for Natural Computing. *Nanotechnology*, **26**, Article ID: 204003. https://doi.org/10.1088/0957-4484/26/20/204003

[15] Strukov, D., Snider, G., Stewart, D. and Williams, R. (2008) The Missing Memristor Found. *Nature*, **453**, 80-83. https://doi.org/10.1038/nature06932

[16] Hasegawa, T., Nayak, A., Ohno, T., Terabe, K., Tsuruoka, T., Gimzewski, J. and Aono, M. (2011) Memristive Operations Demonstrated by Gap-Type Atomic Switches. *Applied Physics A*, **102**, 811-815. https://doi.org/10.1007/s00339-011-6317-0

[17] Tsuruoka, T., Hasegawa, T., Terabe, K. and Aono, M. (2012) Conductance Quantization and Synaptic Behavior in a Ta_2O_5-Based Atomic Switch. *Nanotechnology*, **23**, Article ID: 435705. https://doi.org/10.1088/0957-4484/23/43/435705

[18] Avizienis, A.V., Sillin, H.O., Martin-Olmos, C., Shieh, H.H., Aono, M., Stieg, A.Z. and Gimzewski, J.K. (2012) Neuromorphic Atomic Switch Networks. *PLoS ONE*, **7**, e42772. https://doi.org/10.1371/journal.pone.0042772

[19] Sillin, H.O., Aguilera, R., Shieh, H., Avizienis, A.V., Masakazu, A., Stieg, A.Z. and Gimzewski, J.K. (2013) A Theoretical and Experimental Study of Neuromorphic Atomic Switch Networks for Reservoir Computing. *Nanotechnology*, **24**, Article ID: 384004. https://doi.org/10.1088/0957-4484/24/38/384004

[20] Stieg, A.Z., Avizienis, A.V., Sillin, H.O., Martin-Olmos, C., Aono, M. and Gimzewski, J.K. (2012) Emergent Criticality in Complex Turing B-Type Atomic Switch Networks. *Advanced Materials*, **24**, 286-293. https://doi.org/10.1002/adma.201103053

[21] Hasegawa, T., Ohno, T., Terabe, K., Tsuruoka, T., Nakayama, T., Gimzewski, J.K. and Aono, M. (2010) Learning Abilities Achieved by a Single Solid-State Atomic Switch. *Advanced Materials*, **22**, 1831-1834. https://doi.org/10.1002/adma.200903680

[22] Ohno, T., Hasegawa, T., Tsuruoka, T., Terabe, K., Gimzewski, J.K. and Aono, M. (2011) Short-Term Plasticity and Long-Term Potentiation Mimicked in Single Inorganic Synapses. *Nature Materials*, **10**, 591-595. https://doi.org/10.1038/nmat3054

[23] Wedig, A., Luebben, M., Cho, D., Moors, M., Skaja, K., Rana, V., Hasegawa, T., Adepalli, K., Yildiz, B., Waser, R. and Valov, I. (2015) Nanoscale Cation Motion in TaO_x, HfO_x and TiO_x Memristive Systems. *Nature Nanotechnology*, **11**, 67-74. https://doi.org/10.1038/nnano.2015.221

[24] Nayak, A., Unayama, S., Tai, S., Tsuruoka, T., Waser, R., Aono, M., Valov, I. and Hasegawa, T. (2018) Nanoarchitectonics for Controlling the Number of Dopant Atoms in Solid Electrolyte Nanodots. *Advanced Materials*, **30**, Article ID: 1703261. https://doi.org/10.1002/adma.201703261

[25] Valov, I. and Kozicki, M.N. (2013) Cation-Based Resistance Change Memory. *Journal of Physics D: Applied Physics*, **46**, Article ID: 074005. https://doi.org/10.1088/0022-3727/46/7/074005

[26] Kaeriyama, S., Sakamoto, T., Sunamura, H., Mizuno, M., Kawaura, H., Hasegawa, T., Terabe, K., Nakayama, T. and Aono, M. (2005) A Nonvolatile Programmable Solid-Electrolyte Nanometer Switch. *IEEE Journal of Solid-State Circuits*, **40**, 168-176. https://doi.org/10.1109/JSSC.2004.837244

[27] Suzuki, A., Tsuruoka, T. and Hasegawa, T. (2019) Time-Dependent Operations in Molecular Gap Atomic Switches. *Physica Status Solidi B Basic Research*, **256**, Article ID: 1900068. https://doi.org/10.1002/pssb.201900068

[28] Nayak, A., Tamura, T., Tsuruoka, T., Terabe, K., Hosaka, S., Hasegawa, T. and Aono, M. (2010) Rate-Limiting Processes Determining the Switching Time in a Ag_2S Atomic Switch. *Journal of Physical Chemistry Letters*, **1**, 604-608. https://doi.org/10.1021/jz900375a

[29] Akou, N., Asai, T., Yanagida, T., Kawai, T. and Amemiya, Y. (2010) A Behavioral Model of Unipolar Resistive RAMs and Its Application to HSPICE Integration. *IEICE Electronics Express*, **7**, 1467-1473.

[30] Sheridan, P., Kim, K., Gaba, S., Chang, T., Chen, L. and Lu, W. (2011) Device and SPICE Modeling of RRAM Devices. *Nanoscale*, **3**, 3833-3840. https://doi.org/10.1039/c1nr10557d

[31] Kubota, H., Hasegawa, T., Akai-Kasaya, M. and Asai, T. (2021) Reservoir Computing on Atomic Switch Arrays with High Precision and Excellent Memory Characteristics. *Journal of Signal Processing*, **25**, 123-126. https://doi.org/10.2299/jsp.25.123